A novel level-based automatic wavelet selection scheme for Partial Discharge measurement

A Novel Level-based Automatic Wavelet Selection Scheme for Partial Discharge Measurement

Jeffery C. Chan, *Student Member, IEEE,* Hui Ma, *Member, IEEE,* Tapan K. Saha, *Senior Member, IEEE, and* Chandima Ekanayake, *Member, IEEE*
School of Information Technology & Electrical Engineering
The University of Queensland
St Lucia, QLD-4072, Australia

Abstract — **Partial Discharge (PD) measurement is widely adopted for assessing the insulation conditions of high voltage (HV) equipments. Wavelet transformation (WT) is one the de-noising techniques to extract PD signals from a variety of environmental noises and interferences. In wavelet-based PD signal de-noising, mother wavelet selection is one of the major challenges. This paper proposes a novel level-based (LB) automatic mother wavelet selection scheme in conjunction with discrete WT (DWT) for PD signal de-noising. The de-noising results on both simulative and measured PD signals showed that the proposed scheme could successfully and consistently extract PD signals from noisy signals and retain their integrity.**

Keywords - ***de-noising, high voltage equipment, partial discharge, wavelet transformation***

I. INTRODUCTION

An unexpected failure of high voltage (HV) equipment can cause blackout to thousand customers and may cost millions for repair/replacement [1, 2]. One of the major causes of HV equipment failures arises from the ageing and degradation of insulation systems [1]. Partial discharge (PD) measurement is widely accepted as a non-destructive and effective technique for on-line monitoring and diagnosis of HV equipment insulation system.

PD is a localized electrical discharge that only partially bridges the insulation between conductors [3, 4]. Once PD occurs, discharge pulses will flow through the insulation system. These pulses will gradually erode the insulating materials and eventually damage the integrity of whole insulation system. A PD measurement system performs the tasks of PD signal acquisition, data analysis, feature extraction, and PD source pattern recognition. One of the major challenges of PD measurement is to effectively extract PD signals from extensive environmental interferences and noises.

The convention methods of extracting PD signals from noisy signals (it is termed as de-noising in this paper) are through either time domain (e.g. adaptive filter) or frequency domain (e.g. fast Fourier transform, FFT). In recent years, wavelet transformation (WT) has been adopted for PD signal de-noising in PD measurement due to its ability in analyzing signals in both time and frequency domains [5-15]. The wavelet-based de-noising scheme involves wavelet decomposition, coefficient thresholding, and signal reconstruction. The proper selection of mother wavelet is one of the major challenges in wavelet-based PD signal de-noising as it can totally distort the signal after transformation.

A number of schemes for mother wavelet selection had been proposed in the literature. In [5-7, 15], mother wavelets were chosen based on the correlations between the candidate mother wavelets and the measured PD signals, which are normally corrupted by noises. Since the correlations are calculated using noise-corrupted PD signals, a high noise level may mislead the mother wavelet selection. In [10], the selection of mother wavelets was based on the highest energy in the approximation coefficient, which is obtained through wavelet decomposition. However, high energy can also reside in other coefficients. Thus, the scheme proposed in [10] may compromise the overall de-noising performance. In [8, 11, 12], the authors selected fixed mother wavelets. Although these wavelets showed reasonable de-noising performance, they may not be able to achieve a consistent performance on the PD signals acquired in other occasions.

This paper proposes a novel level-based (LB) automatic scheme for mother wavelet selection in PD signal de-noising. In this scheme, a series of candidate mother wavelets was adopted and noise-corrupted PD signals were decomposed from the lowest to the highest frequencies. Then, correlation between the coefficient at each decomposition level and the PD signals was calculated for different candidate mother wavelets. A mother wavelet, which is able to produce the highest correlation in the decomposed coefficients will be chosen from the candidate mother wavelets and used for PD signal de-noising.

II. REVIEW OF WAVELET TRANSFORMATION (WT) AND MOTHER WAVELET SELECTION FOR PD SIGNAL DE-NOISING

A. Brief review of Wavelet Transformation (WT)

Wavelet is a small wave-type signal with limited time duration and zero-mean in amplitude. It can also be called mother wavelet that satisfies: (i) Total area under the curve of wavelet is zero, $\int_{-\infty}^{\infty}\psi(t)dt = 0$, and (ii) Total area of $|\psi(t)|^2$ is finite, $\int_{-\infty}^{\infty}|\psi(t)|^2 dt < \infty$, where ψ is the mother wavelet [16]. There are many types of mother wavelets and the most commonly adopted wavelets in PD de-noising include Daubechies (db), Biorthogonal (bior), and Coiflets (coif) [5-15].

After selecting the mother wavelet, WT transforms a signal into wavelet coefficients using a shifted and scaled mother wavelet as defined by [16]:

$$\psi_{a,b}(t) = \frac{1}{\sqrt{|a|}}\psi(\frac{t-b}{a}) \quad (1)$$

where a is scale factor and b is translation factor. The scale factor is for compressing and stretching the mother wavelet while the translation factor is for shifting the mother wavelet along the time axis.

In continuous wavelet transformation (CWT), both scale and translation factors change continuously as [16]:

$$W_{a,b} = \int_{-\infty}^{\infty} X(t)\frac{1}{\sqrt{|a|}}\psi^*(\frac{t-b}{a})dt \quad (2)$$

where $X(t)$ is the function of a signal and $\psi*$ is the complex conjugate of mother wavelet. The inverse CWT (ICWT) can be used to reconstruct the signal as [16]:

$$\mathrm{X(t)} = \frac{1}{C}\int_{-\infty}^{\infty}\int_{-\infty}^{\infty} W_{a,b}\psi_{a,b}(t)db\frac{da}{a^2} \quad (3)$$

where C is a constant dependent on the selected mother wavelet. However, CWT is time-consuming since it needs to compute wavelet coefficients at every scale. Also, many redundant signal components can be generated during the calculation. To overcome the above limitations of CWT, discrete wavelet transformation (DWT) has been widely adopted in real applications. DWT can be defined as [16]:

$$W_{j,k} = \sum_{n\in Z} X(n)2^{(-j/2)}\psi(2^{-j}n-k) \quad (4)$$

where $X(n)$ is the discrete function of a signal, j and k are integers. The inverse DWT (IDWT) can be defined as [16]:

$$X(n) = \sum_{j\in Z}\sum_{k\in Z} W_{j,k}\psi_{j,k}(n) \quad (5)$$

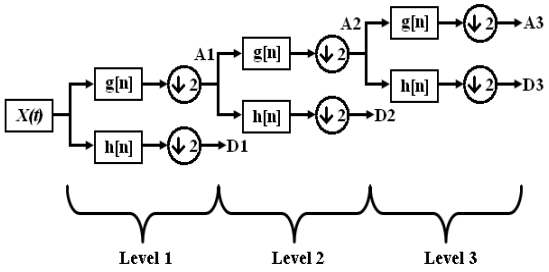

Figure 1. DWT decomposition at level 3 [18] (g[n] and h[n] are LPF and HPF respectively, and A is approximation coefficient and D is detail coefficient)

Figure 1 shows the DWT decomposition [18]. In this figure, a signal is gone through a series of low pass filters (LPFs) and high pass filters (HPFs) and thus it is decomposed into a number of approximation and detail coefficients [17]. Mother wavelet is used to adjust the filtering performance of each filter. Then, both coefficients will be down-sampled and the approximation coefficient will further be decomposed until reaching the predefined decomposition levels. Since on-line PD monitoring requires a relatively fast signal processing technique, this paper will adopt DWT for its efficiency compared to CWT.

B. Review of Existing Mother Wavelet Selection Schemes for PD Signal De-noising

Mother wavelet selection is one of the major tasks in wavelet-based PD signal de-noising. If the selected mother wavelet has high correlation with the real PD signals, better de-noising performance can be achieved. Otherwise, the filters in WT cannot decompose the original noise-corrupted PD signals properly and may lead to poor de-noising performance.

In the literature, some authors used fixed mother wavelets such as db5 and bior1.5 for PD signal de-noising and their results showed that PD signals can be extracted from noisy signals [8, 11, 12]. However, PD is stochastic in nature and there exists various types of PD signals with different properties (i.e. PD pulses shapes and durations). And a homogeneous mother wavelet may not be able to effectively extract PD signals in all occasions. In [13], the author proposed to select mother wavelets based on simulative PD signals. However, since the simulative signals may not match the real PD signals, such approach may exhibit some limitations. In [9], the selection of mother wavelet is based on trial and error. Though this scheme may select the optimal mother wavelet, it is time consuming and may not be used in real time PD measurement.

On the other hand, other researches proposed several mother wavelet selection schemes based on the correlations between the candidate mother wavelets and the original PD signals [5-7, 15]. Ideally, the mother wavelet having higher correlation with a real PD signal will be selected and it is expected to provide better de-noising performance. However, in these schemes the correlations are calculated using the noise-corrupted PD signals and not the real PD signals. For the situation where signal-to-noise ratio (SNR) is low, improper selection of mother wavelet by these schemes may be incurred. That is, a mother wavelet may still be bound to poor de-noising performance even it exhibits high correlation with the noise-corrupted PD signals (refer to Section VI of this paper).

In [10], the authors chose optimal mother wavelets based on the highest energy in the approximation coefficients that produced by a number of candidate mother wavelets. It is assumed that real PD signals have higher energy than noises and they locate only in the approximation coefficient. However, this assumption may not hold in some occasions. This can be exemplified in Figure 2, which shows the decomposition results of applying DWT on a simulative signal that combines with two sinusoid waves. It can be seen from the figure that signals not only locate in approximation level (A5), but also locate in detail levels (D5 and D4).

Based on the aforementioned drawbacks of mother wavelet selection schemes, this paper proposes an automatic mother wavelet selection with the consideration of the highest correlation with original signals among all decomposed coefficients.

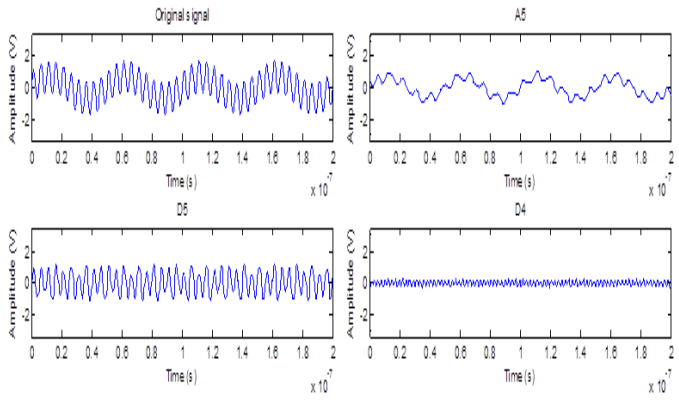

Figure 2. DWT decomposition of a simulative signal at level D4 to A5

III. LEVEL-BASED (LB) AUTOMATIC MOTHER WAVELET SELECTION AND DWT DE-NOSIING SCHEME

This section details a level-based (LB) automatic mother wavelet selection scheme. The proposed scheme is based on the assumption that higher correlation between decomposed coefficients (including both detail and approximation coefficients at every decomposition levels) and original signals can be achieved once an optimal mother wavelet has been found. Differ from the mother wavelet selection scheme propsoed in [10], which selected mother wavelets based on the largest energy located in the approximation coefficient, the scheme proposed in this paper selects an optimal mother wavelet among a series of candidate mother wavelets based on the correlation criterion. The optimal mother wavelet can generate the highest correlation between the decomposed coefficients and original noise-corrupted PD signal. One of the foreseeable advantages of such a scheme is that the mother wavelet selection is not affected by the noises embedded in original signals. Moreover, the proposed LB scheme does not confine the selection only in the approximation coefficient since it calculates the correlations in both approximation and detail coefficients at each decomposition level.

In the above proposed scheme, the threshold values are decided using the method commonly adopted in PD de-noising [5-8, 10-12] :

$$Thr = \frac{m_j}{0.6745} * \sqrt{2 * log(n_j)} \qquad (6)$$

where m_j is the median value of coefficient and n_j is the length of coefficient. The 0.6745 is a rescaling factor that was selected to make the equation suited for Gaussian white noise model [8].

Figure 3 shows the flowchart of the proposed mother wavelet selection scheme. Firstly, the acquired noise-corrupted PD signals are decomposed by DWT with decomposition level five. In this paper, nine mother wavelets including db2, db4, db5, db10, db25, db45, bior1.5, bior6.8, and coif5 were chosen as the candidate mother wavelets (mother wavelet library). For each candidate mother wavelet, the highest correlation between coefficients and original measured PD signals is recorded. And the mother wavelet that attains the highest correlation value among the candidate mother wavelets will be selected as the optimal mother wavelet. After deciding the optimal mother wavelet, threshold will be calculated (Equ. (6)) and applied to each coefficient, which is decomposed by DWT using the optimal mother wavelet. The coefficients which amplitudes are higher than the calculated thresholds will be set to zero. Finally, the de-noised signal can be obtained by reconstructing the thresholded coefficients.

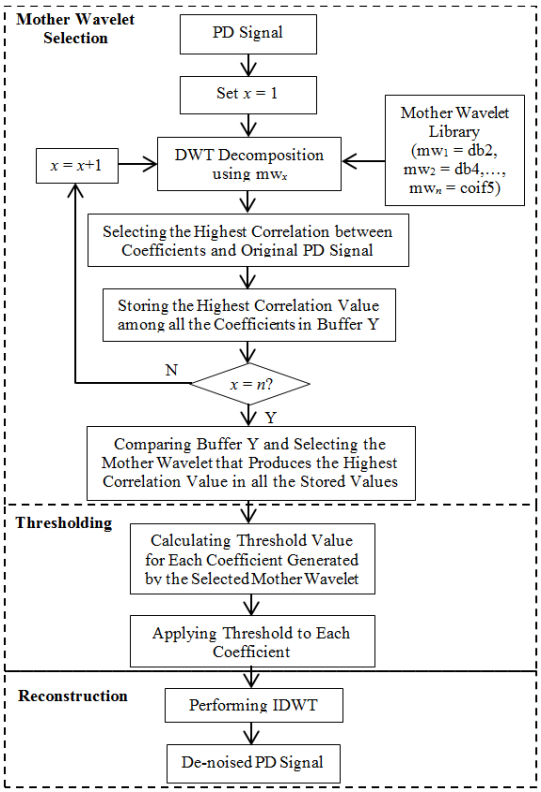

Figure 3. Flowchart of the proposed scheme

IV. EXPERIMENTAL SETUP

Figure 4 depicts the experimental setup for PD measurement [3]. A commercial available PD equipment (Omicron, MPD600), which complies with IEC60270 was used in the experiment.

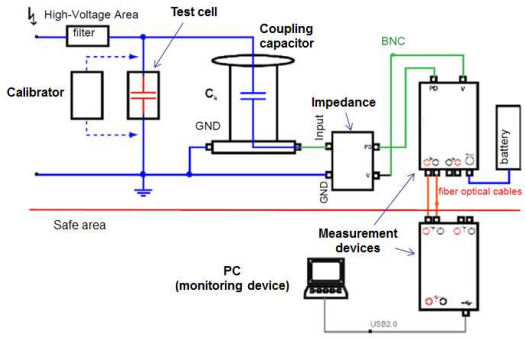

Figure 4. PD mesurements setup [3]

In the experiment, three types of PD source models were designed (

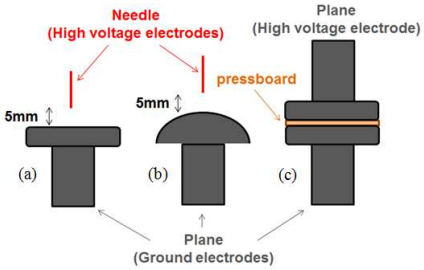

Figure 5). All these models were put into a test cell and immersed in mineral oil. Model 1 is a needle-plane configuration with 5mm between the metal needle (HV electrode) and the copper plane (grounding). Model 2 is a needle-sphere configuration model with 5mm between the metal needle (HV electrode) and the copper sphere (grounding). Model 3 is a 2-plane configuration model with a pressboard (has a small void in the center) between two copper planes with the upper plane is HV electrode and the lower plane is grounding. The pressboard was immersed in mineral oil over 24 hours before commencement of PD measurement.

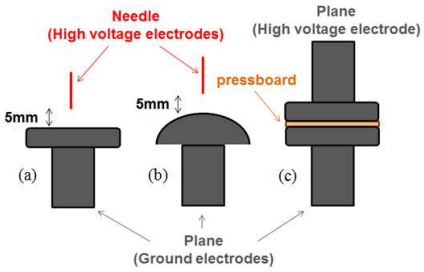

Figure 5. Three different types of models used in PD measurements (a) Model 1, (b) Model 2, and (c) Model 3

V. Simulative and Measured PD Signals

A. Simulative PD Signals

For evaluating the de-noising performance of the proposed scheme, two types of simulative PD signals namely damped exponential pulse (DEP) and damped oscillatory pulse (DOP) were adopted [7] and defined as:

$$\mathrm{DEP(t)} = \mathrm{A}(\mathrm{e}^{-\mathrm{t}/\mathrm{t1}} - \mathrm{e}^{-\mathrm{t}/\mathrm{t2}}) \tag{7}$$

$$\mathrm{DOP(t)} = \mathrm{A} * \sin(2\pi \mathrm{fct})(\mathrm{e}^{-\mathrm{t}/\mathrm{t1}} - \mathrm{e}^{-\mathrm{t}/\mathrm{t2}}) \tag{8}$$

where A is the amplitude of signal, t is time constant, and f_c is oscillatory frequency of DOP. The PD parameters such as rise time, pulse width, and decay time are controlled by the time constant. Figure 7(a) and Figure 8(a) show five of these two types of PD pulses with different amplitudes.

B. Measured PD Signals

PD signals were collected from the three PD source models (Figure 5) when the applied AC voltages (8 kV, 10 kV, and 5 kV for model 1, 2, and 3) exceeded the PD inception voltages. 25 AC cycles of PD signals were extracted for analysis as shown in Figure 6.

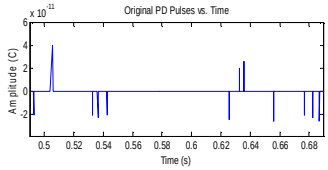

(a) PD signal from model 1

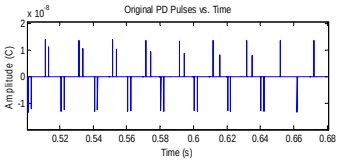

(b) PD signal from model 2

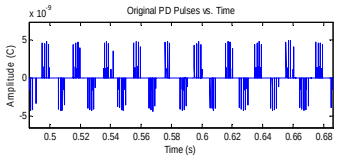

(c) PD signal from model 3

Figure 6. Measured PD signals generated by the three models

It can be seen from the figure that three models produce totally different PD patterns. Therefore, if fixed mother wavelets are applied to the wavelet de-noising for all PD signals, they cannot match the PD signals and a reasonable de-noising performance cannot be ensured.

VI. Evaluation of the Proposed Scheme on PD Signal De-noising

Two commonly used mother wavelet selection schemes in PD signal denoising, the fixed mother wavelet selection scheme (named as F-MWS) and the mother wavelet selection scheme based on correlation with original noise-corrupted PD signals (named as C-MWS), were employed to compare with the proposed scheme in this section.

A. Performance Evaluation Creteria

To verify the performance of the proposed scheme on PD signal de-noising, this paper adopts mean square error (MSE) and correlation coefficient (CC) as performance evaluation measures. MSE and CC are defined as follows:

$$MSE = \frac{1}{N}\sum_{i=1}^{N}(PD_{ori}(i) - PD_{denoi}(i))^2 \tag{1}$$

$$CC = \frac{\sum_{i=1}^{N}(PD_{ori}(i) - \overline{PD_{ori}})(PD_{denoi}(i) - \overline{PD_{denoi}})}{\sqrt{\sum_{i=1}^{N}(PD_{ori}(i) - \overline{PD_{ori}})^2 \sum_{i=1}^{N}(PD_{denoi}(i) - \overline{PD_{denoi}})^2}} \tag{2}$$

where PD_{ori} is original PD signal, PD_{denoi} is de-noised PD signal, and N is the length of the PD signal.

In performance evaluation, Gaussian white noise was added to both simulative and measured PD signals to examine the de-noising capability with different signal-to-noise ratios (SNRs). The SNR (in dB) is defined as:

$$SNR(dB) = 10 * log_{10}\frac{\sum_{i=1}^{N} {PD_{ori}}^2(i)}{\sum_{i=1}^{N} Noi^2(i)} \tag{3}$$

where *Noi* is the applied noise.

B. *Comparison with Fixed Mother Wavelet Selection Scheme (F-MWS)*

This section compares the de-noising performance of the proposed mother wavelet selection scheme with that of the F-MWS. The proposed wavelet scheme selects an optimal mother wavelet from the nine candidate mother wavelets. Five types of signals including two types of simulative PD signals and three types of measured PD signals were used as test cases.

Figure 7 and Figure 8 show the de-noising results of DOP and DEP respectively, which were made up of five simulative PD pulses. Gaussian white noise was added to both signals as shown in Figure 7(b) and Figure 8(b). In Figure 7, the optimal mother wavelet selected by the proposed scheme was coif5, while db5 was used in F-MWS [12]. It can be seen from the figure that DOP-type PD pulses can be successfully extracted from the noisy signals (SNR = 0) using both the proposed scheme and F-MWS. However, the performance of the proposed scheme is better than that of F-MWS, in which some noises still remained after DWT de-noising by the fixed mother wavelet. Figure 8 shows that the proposed scheme can effectively filter out the severe noises (SNR = -5) and successfully extract the five DEP-type PD pulses. In contrast, F-MWS can only extract four PD pulses and failed to filter out some noises. This proves that the proposed scheme can achieve effective and consistent de-noising results when compared with F-MWS.

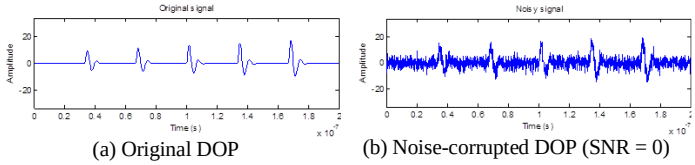

(a) Original DOP (b) Noise-corrupted DOP (SNR = 0)

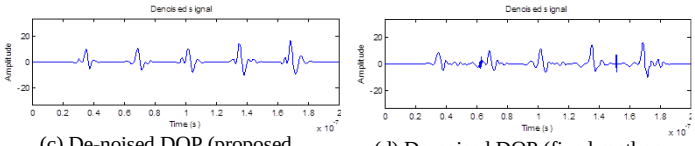

(c) De-noised DOP (proposed scheme: coif5) (d) De-noised DOP (fixed mother wavelet: db5)

Figure 7. Comparison with fixed mother wavelet in DOP

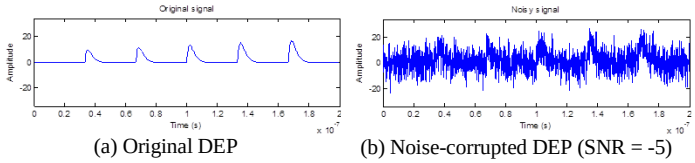

(a) Original DEP (b) Noise-corrupted DEP (SNR = -5)

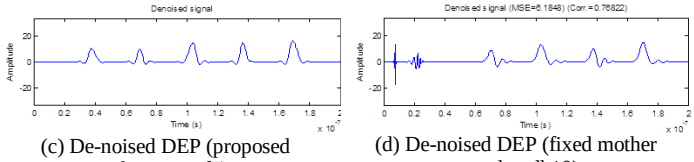

(c) De-noised DEP (proposed scheme: coif5) (d) De-noised DEP (fixed mother wavelet: db10)

Figure 8. Comparison with F-MWS in DEP

Figure 9 presents the de-noising results of the measured PD signal for both proposed scheme and F-MWS. In the figure, the PD signal was acquired by using the experimental setup with test model 1 as described in Section IV. Gaussian white noise (SNR = 3) was added to the measured PD signal to verify the de-noising performance of the two schemes. In F-MWS, wavelet db20 was adopted. In the proposed scheme, the selected optimal mother wavelet was db2. It can be observed from the time diagram of Figure 9(c) (left-hand side of the figure) that the proposed scheme preserves the information of the original measured PD signals after de-noising. In contrast, F-MWS misses some PD pulses and distorts the shape and amplitudes of the pulses after de-noising (left-hand side of Figure 9(d)). The same phenomenon can also be observed in the phase diagram (right-hand side of the same figure) that the amplitudes of some major PD pulses (the black dots) are suppressed and distorted by F-MWS. The similar results can be observed in the measured PD signals using other two models.

Table I shows MSE and CC, which were used as the performance measures for both proposed scheme and F-MWS. In the table, "↓ of MSE (%)" refers to the percentage of MSE reduction from the noise-corrupted signal to the de-noised signal, while "↑ of CC (%)" refers to the percentage of CC increment from the noise-corrupted signal to the de-noised signal. It can be seen from the table that in all cases the MSE reductions in the proposed scheme are more than those in the F-MWS. The largest difference between two schemes is associated with model 1, in which the proposed scheme has 48% MSE decrease and the F-MWS has 22% MSE increase. This corresponds to the case that some PD pulses cannot be extracted in F-MWS. It can also be observed that CC increments in the proposed scheme are more than those in F-MWS.

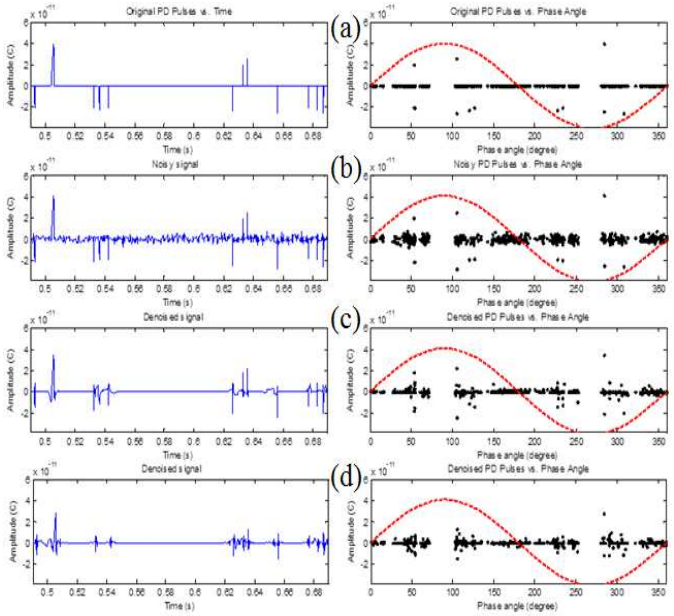

Figure 9. Comparison with F-MWS in model 1 (left: PD signals vs. time, right: PD signals vs. phase angle) (a) original measured PD signal, (b) noise-corrupted PD signal (SNR = 3), (c) de-noising results of the proposed scheme (optimal mother wavelet is db2), and (d) de-noising results of the fixed mother wavelet db20.

Table I. COMPARISON OF MEASURES

	Fixed mother wavelet		Proposed scheme	
	↓ of MSE (%)	↑ of CC (%)	↓ of MSE (%)	↑ of CC (%)
DOP	84	31	92	37
DEP	88	79	95	91

Model 1	-22	-22	48	6
Model 2	65	13	85	35
Model 3	12	-14	55	8

From the above results, it can be concluded that F-MWS cannot effectively remove the noises and retain the original PD signals. This is due to the fact that a fixed mother wavelet may not be able to fully represent different PD signals obtained from different types of PD sources. In contrast, the proposed scheme shows promising results in removing the noises and retaining the PD signals.

C. Comparison with Mother Wavelet Selection Scheme based on Correlation with Original Noise-corrupted PD Signals (C-MWS)

This section provides a comparison between the proposed scheme and C-MWS, which choses mother wavelets based on the calculation of correlations between mother wavelets and original noise-corrupted signals. The correlations between mother wavelets and the signals are obtained by following steps (S1 to S9):

S1) Selecting a mother wavelet in the mother wavelet library.
S2) Normalizing the selected mother wavelet and the original noise-corrupted PD signal in [-1, 1].
S3) Measuring the length (or sample), mw, of the selected mother wavelet, and the length (or sample), pd, of the PD signal.
S4) Setting S = 1 for sample number and C = 0 for the value of correlation.
S5) Extracting the PD signal from samples S to (S-1+ mw).
S6) Calculating correlation, co, between the extracted PD signal and the mother wavelet using Equ. (2).
S7) C = C + co and S = S +1
S8) Go to Step 4 if S < pd-mw+1
S9) C is the correlation between the mother wavelet and the PD signal.

Figure 10(a) shows the correlations and de-noising performance evaluation measures on the simulative DOP-type PD signal, while Figure 10 (b) shows the results of the measured PD signal with test model 1. In both figures, the yellow arrows indicate the mother wavelets that were selected by the proposed scheme and the gray arrows indicate the mother wavelets that were selected by C-MWS.

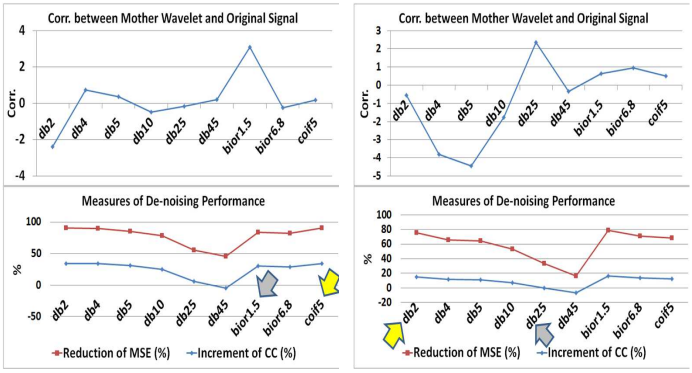

(a) (b)

Figure 10. Comparison with C-MWS in: (a) DOP (SNR = 0) and (b) model 1 (SNR = 3)

It can be observed from the figure that higher correlation values between the mother wavelets and original noise-corrupted PD signals cannot always guarantee the better de-noising performance. For example, in Figure 10(a) the lowest correlation is db2. However, this mother wavelet leads to the largest reduction in MSE and increment in CC. This indicates that even db2 has the lowest coerrelation with the original PD signal, it can still embrace the best de-noising performance compared with other mother wavelets. The C-MWS chose bior1.5 as mother wavelet, while the proposed scheme chose coif5 as optimal mother wavelet. It can be seen from the figure, the de-noising performance of the proposed scheme is better than that of C-MWS. Figure 10(b) compares the de-noising performance of the above two schemes on the measured PD signal. The same result can be revealed from the figure that the proposed scheme still outperforms the C-MWS in terms of MSE reduction and CC increment.

VII. CONCLUSION

Wavelet transformation is one of the de-noising techniques that has been applied in PD measurement. In wavelet PD de-noising, the mother wavelet selection is an imperative task. This paper developed a novel automatic LB mother wavelet selection scheme, which selects mother wavelets based on the highest correlation with original PD signals in all detail and appoximation coefficients at every decomposition level from a series of candidate mother wavelets. The results on both simulative and measured PD signals show that the proposed scheme can successfully extract PD signals from noisy signals with different SNRs. It also shows that the proposed scheme can attain consistent and better de-noising performance compared with other mother wavelet selection schemes proposed in the literature.

REFERENCES

[1] Wang M., Vandermaar A., and Srivastava K., "Review of condition assessment of power transformers in service," IEEE Electrical Insulation Magazine, vol. 18, pp. 12-25, 2002.
[2] Sparling B., "Transformer monitoring and diagnostics," IEEE Power Engineering Society 1999 Winter Meeting, New York, USA, pp. 978-980, 1999.
[3] IEC, "High-voltage test techniques - partial discharge measurements," IEC 60270 International standard, 2000.
[4] Stone G., "Partial discharge diagnostics and electrical equipment insulation condition assessment," IEEE Transactions on Dielectrics and Electrical Insulation, vol. 12, pp. 891-903, 2005.
[5] Ma X., Zhou C., and Kemp I., "Automated wavelet selection and thresholding for PD detection," IEEE Electrical Insulation Magazine, vol. 18, pp. 37-45, 2002.
[6] Zhou X., Zhou C., and Kemp I., "An improved methodology for application of wavelet transform to partial discharge measurement dienoising," IEEE Transactions on Dielectrics and Electrical Insulation, vol. 12, pp. 586-594, 2005.
[7] Ma X., Zhou C., and Kemp I., "Interpretation of wavelet analysis and its application in partial discharge detection," IEEE Transactions on Dielectrics and Electrical Insulation, vol. 9, pp. 446-457, 2002.
[8] Zhang H., Blackburn T., Phung B., and Sen D., "A novel wavelet transform technique for on-line partial discharge measurements part 1: WT de-noising algorithm," IEEE Transactions on Dielectrics and Electrical Insulation, vol. 14, pp. 3-14, 2007.
[9] Gaouda A., Ei-Hag A., Abdel-Galil T., Salama M., and Bartnikas R., "On-line detection and measurement of partial discharge signals in a noisy environment," IEEE Transactions on Dielectrics and Electrical Insulation, vol. 15, pp. 1162-1173, 2008.

[10] Li J., Jiang T., Grzybowski S., and Cheng C., "Scale dependent wavelet selection for de-noising of partial discharge detection," IEEE Transactions on Dielectrics and Electrical Insulation, vol. 17, pp. 1705-1714, 2010.
[11] Zhang H., Blackburn T., Phung B., and Sen D., "A novel wavelet transform technique for on-line partial discharge measurements part 2: on-site noise rejection application," IEEE Transactions on Dielectrics and Electrical Insulation, vol. 14, pp. 15-22, 2007.
[12] Song X., Zhou C., Hepburn D., and Zhang G., "Second generation wavelet transform for data denoising in PD measurement," IEEE Transactions on Dielectrics and Electrical Insulation, vol. 14, pp. 1531-1537, 2007.
[13] Zhongrong X., Ju T., and Caixin S., "Application of complex wavelet transform to suppress white noise in GIS UHF PD signals," IEEE Transactions on Power Delivery, vol. 22, pp. 1498-1504, 2007.
[14] Dey D., Chatterjee B., Chakravorti S., and Munshi S., "Cross-wavelet transform as a new paradigm for feature extraction from noisy partial discharge pulses," IEEE Transactions on Dielectrics and Electrical Insulation, vol. 17, pp. 157-166, 2010.
[15] Chang C., Jin J., Kumar S., Su Q., Hoshino T., Hanai M., and Kobayashi N., "Denoising of partial discharge signals in wavelet packets domain," IEE Proc. Science, Measurement and Technology, vol. 152, pp. 129-140, 2005.
[16] Salomon D., Motta G., and Bryant D., Data compression: the complete reference - ed.4, London: Springer, 2007.
[17] Mallat S., "A theory for multiresolution signal decomposition: the wavelet representation," IEEE Transactions on Pattern Analysis and Machine Intelligence, vol. 11, pp. 674-693, 1989.
[18] Chan J., "Empirical mode decomposition based novel data compression algorithm for wireless data transmission in machine health monitoring," M.Phil. Thesis, City University of Hong Kong, 2009.